Non-Binary LDPC Coded DPSK Modulation for Phase Noise Channels

Tudor Ninacs*, Balázs Matuz*, Gianluigi Liva*
*Institute of Communication and Navigation
Deutsches Zentrum für Luft- und Raumfahrt (DLR), 82234 Wessling, Germany
e-mail: {tudor.ninacs, balazs.matuz, gianluigi.liva}@dlr.de
Giulio Colavolpe†
† Dipartimento di Ingegneria dell'Informazione, Università di Parma 43124, Parma, Italy
e-mail: giulio@unipr.it

***Abstract*—In this paper, we study digital transmission over an additive white Gaussian noise (AWGN) channel with m-ary differential phase-shift keying (DPSK) modulation in the presence of phase noise. At the receiver side, non-coherent iterative detection and decoding is assumed. We present a non-binary low-density generator matrix (LDGM) code design which is suitable for both coherent and non-coherent channels. The code construction is strongly related to the one of non-binary irregular repeat-accumulate (IRA) low-density parity-check (LDPC) codes.**

I. Introduction

In the presence of phase noise, detection may turn out to be a challenging task. Examples are satellite communications in Q/V bands, systems with terminals using cheap oscillators, and/or systems where short message blocks are employed and the use of pilots is limited. In all these cases non-coherent detection is a viable option [1]–[4]. A common technique on non-coherent channels is to employ a differential modulation scheme, particularly in combination with phase-shift keying (PSK). To this end, the PSK modulated symbols are further input to a phase-accumulator before being sent on the channel. At the receiver, non-coherent detectors working on multiple symbols are shown to close the gap w.r.t. ideal coherent detection [2] for sufficiently long sequences.

Whenever channel coding is also considered, iterative detection and decoding at the receiver is a common choice [3]. The schemes for iterative detection/decoding may be divided into two groups [4]. For the first group, standard binary channel codes are complemented by a further block, for instance by the aforementioned differential modulator, in order to compensate for the phase uncertainties from the channel. This results in an iterative demodulation and decoding scheme, as described in [5] and the references therein, which de facto corresponds to a serial turbo(-like) code for which both component codes exchange soft information. High coding gains have been demonstrated with such schemes, e.g., on non-coherent [3], [5] and fading [6] channels.

For the second group of algorithms, one may modify the component decoders/structure of the channel code itself to cope with phase uncertainties. In [7] non-binary low-density parity-check (LDPC) codes over fields were shown to help resolve the unknown phase on the blockwise non-coherent additive white Gaussian noise (AWGN) channel. In [8] LDPC codes were constructed over rings and used for an AWGN channel with phase noise. It has been illustrated for quaternary phase-shift keying (QPSK) modulations that, given a certain partitioning of the check nodes in local and global check nodes, moderate phase noise can be handled with degradations in performance of roughly 0.7 dB.

When PSK modulations are considered, it seems to be natural to use channel codes over rings, preserving the linearity of the overall scheme. Convolutional codes over rings for AWGN channels in absence of phase noise were considered in [9], [10]. LDPC codes over rings for the coherent AWGN channel and PSK modulation were investigated in the context of bandwidth-efficient communications in [11] and it was shown that they may outperform typical techniques like binary bit-interleaved coded modulation. It was noted that the construction of such LDPC codes must be taken with particular care. Zero divisors in the parity-check matrix may lead to poor minimum distances [9].

In this paper, we consider AWGN channels *with* phase noise which we model as a random-walk process using the Wiener model. We propose a scheme that is a serial concatenation of two component codes: an outer non-binary low-density generator matrix (LDGM) code over a field of order m and an inner accumulator over the ring of integers modulo m. The concatenated scheme resembles an LDPC code with accumulator structure whose output serves as input to a m-PSK modulator. At the receiver, demodulation and decoding of the inner component code are done jointly using a discretized-phase (DP) detection algorithm [12], whereas the outer component code is decoded by belief propagation (BP) on the outer code's bipartite graph. Note that a related concept of joining detector and check node decoder for *binary* repeat-accumulate (RA) codes was introduced for multiple-input and multiple-output (MIMO) communication links in [13] and adopted to

This work has been accepted for publication at the IEEE International Conference on Communications 2017, IEEE ICC'17: Bridging People, Communities, and Cultures.

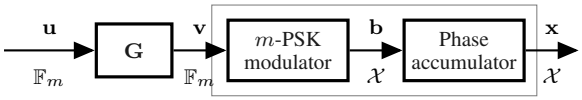

Fig. 1: Transmitter of the proposed scheme.

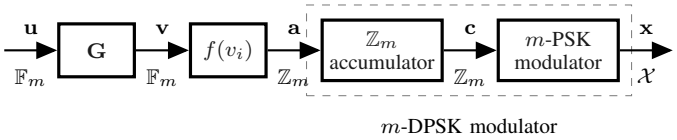

Fig. 2: Equivalent transmitter description.

channels with phase noise in [14].

II. Preliminaries

We consider transmission over an AWGN channel with phase noise and assume m-ary differential phase-shift keying (DPSK) at the transmitter. Denote the vector of received samples by $\mathbf{r} = [r_0, \ldots, r_N]$ and the vector of modulated codeword symbols by $\mathbf{x} = [x_0, \ldots, x_N]$. In the discrete-time baseband model, the relation between the transmitted and received symbols can be expressed as

$$\begin{aligned} r_i &= x_i e^{j\theta_i} + n_i \\ &\overset{(1)}{=} e^{j\phi_i} e^{j\theta_i} + n_i \\ &\overset{(2)}{=} e^{j\psi_i} + n_i \end{aligned}$$

where (1) is due to the use of m-DPSK modulation, for which $x_i = e^{j\phi_i}$, $\phi_i \in \{2\pi l/m\}$, with $l \in \{0, \ldots, m-1\}$. Further, (2) results from the definition $\psi_i = [\theta_i + \phi_i]_{2\pi}$, having denoted by $[\cdot]_{2\pi}$ the operation modulo 2π. We have that n_i are independent complex Gaussian noise samples, i.e., $n_i \sim \mathcal{CN}(0, 2\sigma^2)$ and the channel phase noise is modeled according to the Wiener model with

$$\theta_i = \theta_{i-1} + \Delta\theta_i, \tag{1}$$

where $\Delta\theta_i \sim \mathcal{N}(0, \sigma_\Delta^2)$, θ_0 being uniformly distributed in $[0, 2\pi)$.

In Section VI, we also present results for a *blockwise* non-coherent AWGN channel which is obtained by setting $\sigma_\Delta^2 = 0$. In this case the phase is constant, but unknown and uniformly distributed in $[0, 2\pi)$ over an entire codeword, and we have

$$r_i = x_i e^{j\theta} + n_i.$$

III. Transmitter Description

A. Proposed Scheme

Figure 1 depicts the transmitter of the proposed scheme. It consists of the serial concatenation of a (N, K) linear block code $\mathcal{C}$ over $\mathbb{F}_m$ and a m-DPSK modulator. Throughout the entire manuscript we will consider $m = 2^p, p \in \mathbb{N}, p > 1$. Denoting by $\mathbf{G}$ the $K \times N$ generator matrix of $\mathcal{C}$, we have that the input vector $\mathbf{u} = [u_1, \ldots, u_K]$ is encoded into an (outer) codeword $\mathbf{v} = [v_1, \ldots, v_N]$ with $\mathbf{v} = \mathbf{uG}$. The symbols v_i are then input to a m-DPSK modulator, which first maps each v_i to a complex m-PSK symbol $b_i = e^{j\varphi_i}$, with $\mathbf{b} = [b_1, \ldots, b_N]$, and then accumulates the phases, yielding the modulated codeword symbols $\mathbf{x} = [x_0, \ldots, x_N]$. By defining the channel input alphabet $\mathcal{X} = \left\{e^{j2\pi l/m}\right\}$, $l \in \{0, \ldots, m-1\}$ we have that $b_i, x_i \in \mathcal{X}$. Note that the phase accumulator outputs $N+1$ symbols x_i, where $x_0 = 1$.

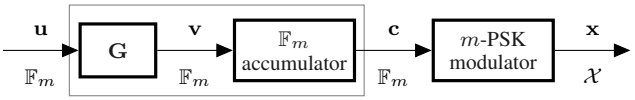

Fig. 3: Structure of a non-systematic IRA encoder with m-PSK.

The scheme admits an equivalent representation which is provided in Figure 2. For this, assume that in an intermediate step the symbols $v_i \in \mathbb{F}_m$ are mapped by a bijective function $f : \mathbb{F}_m \to \mathbb{Z}_m$ to symbols $a_i \in \mathbb{Z}_m$, i.e., to elements of the ring of integers modulo m. For the m-DPSK constellation labels we consider Gray mapping and define the bijective mapping f so that the binary representations of the $\mathbb{F}_m$ elements match the labels of the m-DPSK constellation points. E.g. for $m = 8$, the mapping f is specified in Table I. Using $\arg(b_i) = \varphi_i = 2\pi a_i/m$ and $\phi_i = \phi_{i-1} + \varphi_i$, x_i equals

$$x_i = e^{j\phi_i} = e^{j\sum_{l=1}^{i}\varphi_l} = e^{j2\pi/m\sum_{l=1}^{i} a_l} \tag{2}$$

where without loss of generality $\phi_0 = 0$. Next, the order of the blocks inside the m-DPSK modulator in Figure 1 is reversed so that symbols a_i are first input to an accumulator over $\mathbb{Z}_m$ and afterwards to the m-PSK modulator. In particular, the accumulator computes the output symbol at time i as

$$c_i = c_{i-1} + a_i = \sum_{l=1}^{i} a_l$$

where the sum is defined over $\mathbb{Z}_m$ and $c_0 = 0$. Now, by mapping c_i to a m-PSK constellation point, we obtain

$$x_i = e^{j\phi_i} = e^{(j2\pi c_i/m)} = e^{j2\pi/m\sum_{l=1}^{i} a_l}$$

which is identical to (2) and illustrated in Figure 2.

Figure 2 allows a different interpretation of the encoder. In fact, we can regard the serial concatenation of the (outer) code $\mathcal{C}$ and the (inner) accumulator over $\mathbb{Z}_m$ as a block code with input $\mathbf{u}$ defined over $\mathbb{F}_m$ and output $\mathbf{c}$ defined over $\mathbb{Z}_m$. This is very reminiscent, though not equivalent, of the structure of a non-systematic irregular repeat-accumulate (IRA) [15] code over $\mathbb{F}_m$ as in Figure 3. The scheme in Figure 3 is not meant for transmission over non-coherent channels. Nevertheless, we exploit the similarities to construct the code $\mathcal{C}$ for the m-DPSK coded scheme under the assumption of iterative decoding and detection.

B. Reference Scheme

In the sequel a competing state-of-the-art scheme from the literature [4] will be also considered and its performance presented in Section VI. It is obtained by replacing the outer code $\mathcal{C}$ in Figure 2 by a *binary* convolutional code with generator polynomials $(7, 5)$ in octal notation, as described

TABLE I: Mapping between field elements, their binary representation, ring elements and modulation symbols with $m = 8$. The primitive polynomial for $\mathbb{F}_8$ is $1 + \mathrm{x} + \mathrm{x}^3 = 0$.

$\mathbb{F}_8$ element	Binary label	$\mathbb{Z}_8$ element	8-PSK symbol
0	000	0	0
α^0	001	1	$e^{j\pi/4}$
α^1	010	3	$e^{j3\pi/4}$
α^2	100	7	$e^{j7\pi/4}$
α^3	011	2	$e^{j\pi/2}$
α^4	101	6	$e^{j3\pi/2}$
α^5	111	5	$e^{j5\pi/4}$
α^6	110	4	$e^{j\pi}$

in [4]. Further, the scheme is complemented by an interleaver which acts on the output bits of the outer code. The interleaved bits are then mapped to $\mathbb{Z}_m$ by a mapping function and passed to the inner encoder, i.e., the $\mathbb{Z}_m$-accumulator.Finally, the symbols are m-PSK modulated. Decoding is performed by iteratively exchanging messages among the inner and outer decoders through an interleaver. The result is a powerful serial turbo scheme [4], [6], [16] to which we will refer as serial turbo code throughout the remaining parts of the paper.

IV. Code Design

A. Review of IRA Codes over $\mathbb{F}_m$

The IRA encoder in Figure 3 works as follows. The information vector $\mathbf{u}$ is first multiplied by the matrix $\mathbf{G}$ yielding the outer codeword $\mathbf{v}$. Symbols of $\mathbf{v}$ are then input to a time-varying accumulator over $\mathbb{F}_m$ which produces the codeword symbols through the recursion

$$c_i = w_i \cdot c_{i-1} + v_i$$

where $(\cdot, +)$ are defined in $\mathbb{F}_m$, $m = 2^p, p \in \mathbb{N}, p > 1$. For the code design, we assume that the multiplicative coefficients used on the feedback branch of the accumulator w_i with $i = 1, \ldots, N-1$, are chosen with uniform probability in $\mathbb{F}_m \backslash \{0\}$. Let us introduce the $N \times N$ double-diagonal matrix $\mathbf{W}$ which has form

$$\mathbf{W} = \begin{bmatrix} 1 & 0 & 0 & \ldots & 0 & 0 & 0 \\ w_1 & 1 & 0 & \ldots & 0 & 0 & 0 \\ 0 & w_2 & 1 & \ldots & 0 & 0 & 0 \\ \vdots & \vdots & \vdots & \ddots & \vdots & \vdots & \vdots \\ 0 & 0 & 0 & \ldots & 1 & 0 & 0 \\ 0 & 0 & 0 & \ldots & w_{N-2} & 1 & 0 \\ 0 & 0 & 0 & \ldots & 0 & w_{N-1} & 1 \end{bmatrix}.$$

The generator matrix of the IRA code $\mathcal{C}_{\mathsf{IRA}}$ is given by

$$\mathbf{G}_{\mathsf{IRA}} = \mathbf{G}(\mathbf{W}^{-1})^{\mathsf{T}}$$

and the codeword $\mathbf{c} = \mathbf{u}\mathbf{G}_{\mathsf{IRA}}$. Consider now a code $\mathcal{C}_{\mathsf{SIRA}}$ obtained by appending to each codeword $\mathbf{c}$ of the IRA the information vector $\mathbf{u}$, producing a new codeword $[\mathbf{u}|\mathbf{c}]$. The code $\mathcal{C}_{\mathsf{SIRA}}$ is an IRA code with systematic encoder, having a generator matrix of the form

$$\mathbf{G}_{\mathsf{SIRA}} = \left[\mathbf{I} \,\middle|\, \mathbf{G}(\mathbf{W}^{-1})^{\mathsf{T}}\right]$$

and parity-check matrix

$$\mathbf{H}_{\mathsf{SIRA}} = \left[\mathbf{G}^{\mathsf{T}} \,\middle|\, \mathbf{W}\right] \tag{3}$$

having denoted by $\mathbf{I}$ a $K \times K$ identity matrix. By construction, the IRA code with non-systematic encoding can be viewed as a punctured version of the IRA code with systematic encoding. Hence, the IRA code with non-systematic encoding can be decoded over the Tanner graph associated to $\mathbf{H}_{\mathsf{SIRA}}$, where the variable nodes associated with the first K columns of $\mathbf{H}_{\mathsf{SIRA}}$ are not connected to the channel.

B. Surrogate Design

To facilitate the code design, we follow a *surrogate* design approach. To this end, we first design the parity-check matrix $\mathbf{H}_{\mathsf{SIRA}}$ of an IRA code over $\mathbb{F}_m$ for the coherent AWGN channel without phase-noise. For this we rely on standard tools from the literature. More precisely, our design is based on protographs which are relatively small bipartite graphs that serve as templates for larger graphs [17]. Suitable protographs can be found, e.g., by density evolution [18] while the progressive edge growth (PEG) algorithm [19] can be used to obtain the Tanner graph of the code. We then adopt the resulting matrix $\mathbf{G}$ to describe the outer code $\mathcal{C}$ in the m-DPSK coded modulation scheme.

More in detail, the code design proceeds by optimizing the protograph structure with respect to the iterative decoding threshold via density evolution analysis. Due to the potentially large search space, one may restrict the optimization to a specific family of IRA protographs. In this paper we focus on IRA protographs with base matrix

$$\mathbf{B}_{\mathsf{SIRA}} = \left[\begin{array}{c|cc} 1 & 1 & 1 \\ d & 1 & 1 \end{array}\right]$$

where the leftmost column of $\mathbf{B}_{\mathsf{SIRA}}$ is associated with the (punctured) systematic part of the codeword, d being a positive integer parameter over which we optimize via Monte Carlo density evolution for the coherent AWGN channel. To handle the lack of symmetry in the codebook stemming from the use of m-PSK modulations with $m > 4$, we resort to the use of channel adapters in the analysis [18]. Note that, for a 2×3 protograph, the freedom in design is limited. The upper 'one' entry in the leftmost column is required for convergence purposes when puncturing. Also, the two rightmost columns have a fixed structure to realize an accumulator. Resulting iterative decoding thresholds for the coherent AWGN channel for various d are depicted in Table II. Following this, we select a protograph with $d = 2$, since simulation results suggest lower error floors than for $d = 1$. Finally, once $\mathbf{H}_{\mathsf{SIRA}}$ is available, the outer code in Figure 2 is obtained by extracting $\mathbf{G}$ from $\mathbf{H}_{\mathsf{SIRA}}$ following Equation (3). Due to the low-density nature of $\mathbf{G}$, the outer code is an LDGM code. Decoding is done via BP on the bipartite graph of the parity-check matrix $\mathbf{H}_{\mathsf{dec}}$ of its systematic counterpart, where $\mathbf{H}_{\mathsf{dec}} = \left[\mathbf{G}^{\mathsf{T}}|\mathbf{I}\right]$ is sparse.

V. Receiver Description

A. Overview

A block diagram of the receiver is given in Figure 4. It consists of an inner decoder, i.e., a m-DPSK detector, as

TABLE II: Iterative decoding thresholds $(E_b/N_0)^*$ for different values of $d$for the coherent AWGN channel. The Shannon limit corresponding to a rate of 1.5 bits per channel use under 8-PSK modulation is at $(E_b/N_0)_{\mathsf{Sh}} = 1.3$ dB.

d	$(E_b/N_0)^*$ [dB]
1	2.1
2	2.2
3	3.1
4	4.0

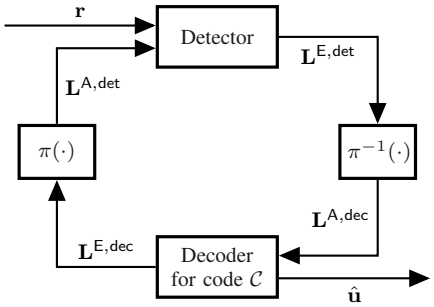

Fig. 4: Structure of the iterative receiver.

well as an outer decoder for the code $\mathcal{C}$ which is decoded by standard BP [20]. The two decoders iteratively exchange soft information. In detail, the received word $\mathbf{r}$ serves as input to a maximum a posteriori (MAP) detector which produces extrinsic soft information $\mathbf{L}_i^{\mathsf{E,det}}$ on the symbols a_i (c.f. Figure 2). We have that

$$\mathbf{L}_i^{\mathsf{E,det}} = \mathbf{L}_i^{\mathsf{APP,det}} \Big/ \mathbf{L}_i^{\mathsf{A,det}}$$

where the division is done element-wise, $\mathbf{L}_i^{\mathsf{APP,det}} = P(a_i|\mathbf{r})$ is a m-dimensional probability mass function (p.m.f.) and $\mathbf{L}_i^{\mathsf{A,det}} = P(a_i)$ is initialized to $[1/m, \ldots, 1/m]$ prior to starting the iterative process and refined iteration by iteration.

The extrinsic information output by the detector is de-permuted by the function $\pi^{-1}(\cdot)$ to obtain the a priori soft information input to the decoder $\mathbf{L}_i^{\mathsf{A,dec}}$. The de-permutation of the p.m.f.s is due to the mapping $f^{-1}(\cdot)$ at the encoder. During the iteration process, the decoder estimates the MAP probability $P(v_i|\mathbf{L}^{\mathsf{A,dec}})$ for the outer code symbols v_i. Only extrinsic information $\mathbf{L}^{\mathsf{E,dec}} = \mathbf{L}_i^{\mathsf{APP,dec}} \Big/ \mathbf{L}_i^{\mathsf{A,dec}}$ on the symbols v_i is forwarded, permuted and provided as a priori information $\mathbf{L}^{\mathsf{A,det}}$ to the detector, where

$$\mathbf{L}_i^{\mathsf{APP,dec}} \approx P(v_i|\mathbf{L}_i^{\mathsf{A,dec}})$$

and $\mathbf{L}_i^{\mathsf{A,det}} = \pi\left(\mathbf{L}_i^{\mathsf{E,dec}}\right)$. Again the permutation of the p.m.f.s is due to the mapping $f(\cdot)$ at the encoder.

An exchange of information between detector and decoder is performed for a maximum number of iterations.[1] Finally, the iterative scheme provides an estimate of $P(u_i|\mathbf{r})$, $\mathbf{L}^{\mathsf{APP}}(u_i) \approx P(u_i|\mathbf{r})$ upon which a decision on the information symbols is made

$$\hat{u}_i = \arg\max_{u_i} P(u_i|\mathbf{L}^{\mathsf{APP}}(u_i)).$$

[1]In this work, we fix the number of internal iterations of the decoder to one and the number of iterations between decoder and detector to 200.

B. Discretized-Phase Algorithm

We now address the operation of the detector. We aim to compute $\mathbf{L}_i^{\mathsf{E,det}} = P(a_i|\mathbf{r})/P(a_i)$ and thus express the joint p.m.f. $p(\mathbf{a}, \boldsymbol{\psi}|\mathbf{r})$ as

$$\begin{aligned} p(\mathbf{a}, \boldsymbol{\psi}|\mathbf{r}) &= p(\mathbf{r}|\mathbf{a}, \boldsymbol{\psi}) p(\boldsymbol{\psi}|\mathbf{a}) P(\mathbf{a}) \frac{1}{p(\mathbf{r})} \\ &\propto p(r_0|\psi_0) \prod_{i=1}^{N} p(r_i|\psi_i) p(\psi_i|\psi_{i-1}, a_i) P(a_i)\,. \end{aligned}$$

Above we have used the fact that due to the Wiener model and the differential modulation $p(\psi_i|\psi_{i-1}, \ldots, \psi_0, \mathbf{a}) = p(\psi_i|\psi_{i-1}, a_i)$. Since the joint p.m.f. $p(\mathbf{a}, \boldsymbol{\psi}|\mathbf{r})$ is given as a product of probabilities, the marginal symbol-wise p.m.f. $P(a_i|\mathbf{r})$ can be computed with the help of a forward/backward recursion on the corresponding factor graph [21] of the function. From this we have that

$$\frac{P(a_i|\mathbf{r})}{P(a_i)} = \int_0^{2\pi}\int_0^{2\pi} \alpha(\psi_{i-1})\beta(\psi_i) p(\psi_i|\psi_{i-1}, a_i) d\psi_i d\psi_{i-1} \quad (4)$$

where $\alpha(\psi_i)$ and $\beta(\psi_i)$ are the forward/backward coefficients obtained from the factor graph as [12]

$$\begin{aligned} \alpha(\psi_i) &= p(r_i|\psi_i) \cdot \\ &\quad \cdot \int_0^{2\pi} \left(\sum_{a_i} p(\psi_i|\psi_{i-1}, a_i) P(a_i) \right) \alpha(\psi_{i-1})\; d\psi_{i-1} \end{aligned} \quad (5)$$

$$\begin{aligned} \beta(\psi_i) &= p(r_i|\psi_i) \cdot \\ &\quad \cdot \int_0^{2\pi} \left(\sum_{a_{i+1}} p(\psi_{i+1}|, \psi_i, a_{i+1}) P(a_{i+1}) \right) \beta(\psi_{i+1})\; d\psi_{i+1}, \end{aligned} \quad (6)$$

with $\alpha(\psi_0) = p(r_0|\psi_0)$ and $\beta(\psi_N) = p(r_N|\psi_N)$.

Next we elaborate on the expressions involved in the computation of the forward/backward coefficients. We have that

$$p(r_i|\psi_i) = \frac{1}{\sqrt{2\pi\sigma^2}} e^{-\frac{|r_i - e^{j\psi_i}|^2}{2\sigma^2}}$$

and from the Wiener model in (1) and the identity $\phi_i = \phi_{i-1} + \varphi_i$, ψ_i can be written as $\psi_i = [\psi_{i-1} + \varphi_i + \Delta\theta_i]_{2\pi}$. Since $b_i = e^{j\varphi_i} = e^{j2\pi a_i/m}$ is a deterministic mapping of a_i, it holds that

$$p(\psi_i|\psi_{i-1}, a_i) = p(\psi_i|\psi_{i-1}, b_i) = p_\Delta(\psi_i - \psi_{i-1} - \varphi_i)$$

where $p_\Delta(\cdot)$ is the probability density function (p.d.f.) of the phase increment $\Delta\theta_i$ in the Wiener process (modulo 2π). Furthermore, we can express

$$p_\Delta(\varphi) = \sum_{\ell=-\infty}^{+\infty} g(0, \sigma_\Delta^2; \varphi - 2\pi\ell) \quad (7)$$

where

$$g(\mu, \sigma_\Delta^2; \varphi) = \frac{1}{\sqrt{2\pi\sigma_\Delta^2}} e^{-\frac{(\varphi-\mu)^2}{2\sigma_\Delta^2}}\,. \quad (8)$$

For practical values of σ_Δ, the tails of the p.d.f. in (8) tend to zero in almost all points except some in the vicinity of μ [14], and we have that

$$p_\Delta(\varphi) \simeq g(0, \sigma_\Delta^2; \varphi)$$

and thus (7) simplifies to

$$p_\Delta(\psi_i - \psi_{i-1} - \varphi_i) \simeq g(0, \sigma_\Delta^2; \psi_i - \psi_{i-1} - \varphi_i)\,. \qquad (9)$$

Even in its simplified form, using (9) in (4), (5) and (6) involves computing integrals of continuous p.d.f.s. A more practical approach is the use of a DP algorithm [4] which assumes ψ_i only takes values in the discrete set $\{2\pi j/L\}$, $j \in \{0, \ldots, L-1\}$, where L is a design parameter. Combined with the fact that for practical values of σ_Δ the p.d.f. in (9) has non-zero values only in the strict vicinity of 0, the following approximation [5] may be used

$$p_\Delta(\varphi) = \begin{cases} 1 - P_\Delta, & \varphi = 0 \\ \frac{P_\Delta}{2}, & |\varphi| = \frac{2\pi}{L} \\ 0, & \text{otherwise} \end{cases}.$$

In accordance with [5], a phase discretization factor of $L = 8m$ has been chosen. The parameter P_Δ is a design parameter, also referred to in literature as transition probability of the discretized model [14]. By using this approximation, the integrals in (4), (5) and (6) become summations and the computation of the forward/backward coefficients, as well as of the extrinsic probabilities becomes practical.

VI. Numerical Results

We target short blocks in the order of a few hundred code bits. We illustrate that, despite the short block-length, the proposed code construction works well on coherent channels, as well as on blockwise non-coherent AWGN channels and AWGN channels with (symbol-wise) phase noise, as described in Section II.

A. Coherent AWGN Channel

In the following, we assume 8-DPSK. We designed an outer LDGM code $\mathcal{C}$ over $\mathbb{F}_8$ following Section IV. Together with the inner code, i.e., the $\mathbb{Z}_8$-accumulator we obtain an LDPC-like code, as pointed out earlier. We focus on short codes with $K = 100$ symbols (300 bits) and $N = 200$ symbols (600 bits). First, the performance of the code on a coherent AWGN channel is presented. For both decoder and detector we used the schemes described in Section V and set the design parameter $P_\Delta = 0.1$ which is compliant with [14]. A consequence of using the DP-detector is a *mismatch* to the channel, since the detector assumes a phase uncertainty which is not present in the coherent case.

As a reference, for the coherent channel we have also simulated the performance of the iterative scheme removing the DP model in the detector. For this, we run BP on the bipartite graph of the outer code $\mathcal{C}$ and of the inner accumulator. This procedure would not work on the phase noise channel and is only shown here to discuss the sub-optimality of the DP algorithm for the selected block length.

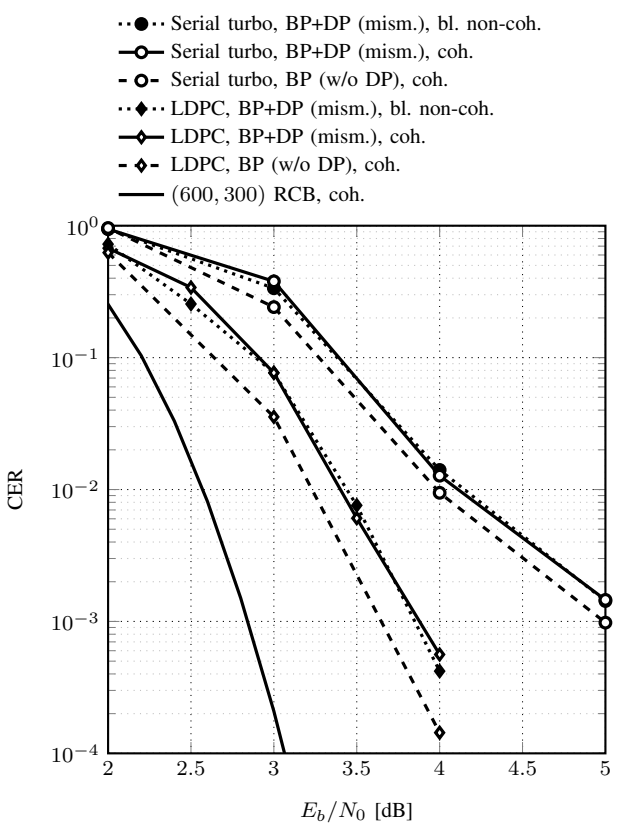

Fig. 5: CER vs. E_b/N_0 of LDPC and serial turbo code on a coherent AWGN channel under BP w/o DP and BP+DP decoding. Also the performance on the blockwise non-coherent AWGN channel under BP+DP decoding is given.

Simulation results in terms of CER versus E_b/N_0 are presented in Figure 5 together with the random coding bound (RCB) [22] as a benchmark. We observe that the proposed scheme is within 1 dB from the corresponding RCB. Further, for the proposed block length, owing to the mismatched DP-detector, a slight loss of 0.2 dB w.r.t. matched detection is visible. Finally, we also simulated the performance of the serial turbo code from Section III-B. Also in this case we assumed both a detector w/o the DP algorithm for the coherent case, as well as a mismatched DP-detector. The turbo code exhibits a further loss of more than 1 dB compared to the proposed construction.

B. Blockwise Non-coherent AWGN Channel

In Figure 5 we have also depicted the performance of the LDPC code on a blockwise non-coherent AWGN channel, for which the phase is unknown, but constant over an entire codeword duration. We assume again the DP-detector in place, yielding a mismatch w.r.t. the channel, since phase transitions among modulation symbols within a codeword are not present. Compared to the coherent setting with perfect phase knowledge one may observe from Figure 5 that the proposed scheme with the DP-detector only loses 0.2 dB, thus yielding approximately the same performance as on the coherent channel. Similarly the turbo code is simulated and a loss in the order of 1 dB w.r.t. the LDPC scheme is visible.

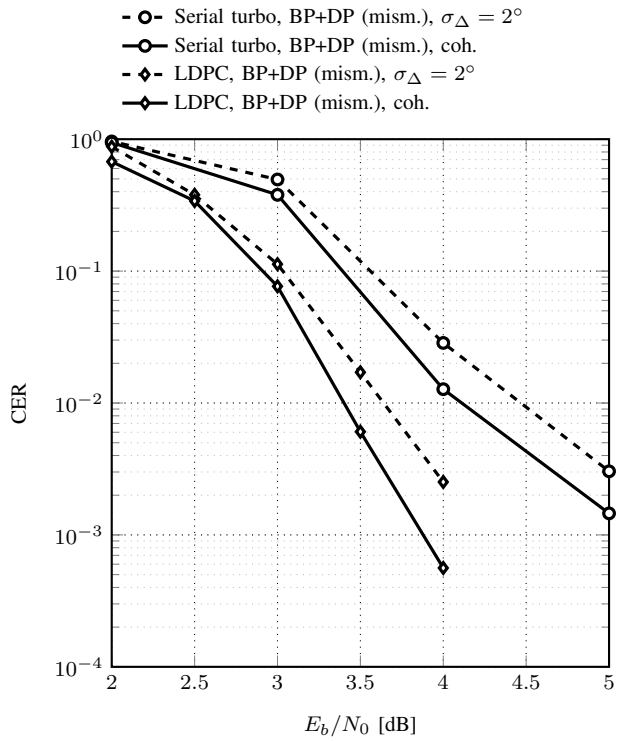

Fig. 6: CER vs. E_b/N_0 of LDPC and serial turbo code on a coherent, as well as non-coherent AWGN channel with $\sigma_\Delta = 2°$.

C. Non-coherent AWGN Channel with Phase Noise

We apply the proposed algorithm on the phase noise channel as described in Section II. We introduce a phase noise with $\sigma_\Delta = 2°$. Note that typical Digital Video Broadcasting Satellite 2 (DVB-S2) consumer grade equipment experiences values smaller than this, e.g. as can be observed by comparing the phase noise mask of DVB-S2 [23] to the power spectral density (PSD) of the Wiener process having $\sigma_\Delta = 2°$. In Figure 6 CER performances are shown, recapping also the results for a coherent AWGN channel with mismatched detection. Observe a loss w.r.t. the coherent case of merely 0.3 dB underlining the robustness of the proposed scheme. Also the performance of the serial turbo code is depicted for the same setting. Also here we experience similar degradation w.r.t. the phase noise free case. Still a gap of around 1 dB compared to the LDPC code remains.

VII. Conclusions

We proposed non-systematic LDGM codes over finite fields $\mathbb{F}_m$ concatenated with m-DPSK modulation, where the field order is matched to the modulation order. To obtain the LDGM code we rely on a surrogate design which is inspired by $\mathbb{F}_m$ IRA LDPC codes. Thanks to its accumulator-based structure, the resulting code concatenation performs well not only on coherent AWGN channels, but also on blockwise non-coherent AWGN channels, as well as on AWGN channels with phase noise. A noticeable gain is experienced w.r.t. standard serial turbo codes.

References

[1] J. Proakis and M. Salehi, *Digital Communications*. New York, NY, USA: McGraw-Hill, 2008.

[2] D. Divsalar and M. K. Simon, "Multiple-symbol differential detection of MPSK," *IEEE Trans. Commun.*, vol. 38, no. 3, pp. 300–308, Mar. 1990.

[3] G. Colavolpe, A. Barbieri, and G. Caire, "Algorithms for iterative decoding in the presence of strong phase noise," *IEEE J. Sel. Areas Commun.*, vol. 23, no. 9, pp. 1748–1757, Sep. 2005.

[4] G. Colavolpe, "Communications over phase-noise channels: A tutorial review," *Int. J. Satell. Commun. Network.*, vol. 32, pp. 167–185, May/Jun. 2014, article first published online: Jul. 2013.

[5] M. Peleg, S. Shamai, and S. Galan, "Iterative decoding for coded noncoherent MPSK communications over phase-noisy AWGN channel," *IEE Proc. Commun.*, vol. 147, no. 2, pp. 87–95, Apr. 2000.

[6] P. Hoeher and J. Lodge, ""Turbo DPSK": iterative differential PSK demodulation and channel decoding," *IEEE Trans. Commun.*, vol. 47, no. 6, pp. 837–843, Jun. 1999.

[7] B. Matuz, G. Liva, E. Paolini, M. Chiani, and G. Bauch, "Low-rate non-binary LDPC codes for coherent and blockwise non-coherent AWGN channels," *IEEE Trans. Commun.*, vol. 61, no. 10, pp. 4096–4107, Oct. 2013.

[8] S. Karuppasami and W. Cowley, "Construction and iterative decoding of LDPC codes over rings for phase-noisy channels," *EURASIP J. Wirel. Commun. Netw.*, vol. 2008, pp. 1–9, Jan. 2008.

[9] R. Filho and P. Farrell, "Coded modulation with convolutional codes over rings," in *Proc. EUROCODE '90*, ser. Lecture notes on computer science, Udine, Italy, Nov. 1990, pp. 271–280.

[10] J. L. Massey and T. Mittelholzer, "Convolutional codes over rings," in *Proc. 4th Joint Swedish-Soviet Int. Workshop on Inf. Theory*, Gotland, Sweden, Aug. 2008, pp. 14–18.

[11] D. Sridhara and T. Fuja, "LDPC codes over rings for PSK modulation," *IEEE Trans. Inf. Theory*, vol. 51, no. 9, pp. 3209–3220, Sep. 2005.

[12] A. Barbieri and G. Colavolpe, "Soft-output decoding of rotationally invariant codes over channels with phase noise," *IEEE Trans. Commun.*, vol. 55, no. 10, pp. 2033–2033, Oct. 2007.

[13] S. ten Brink and G. Kramer, "Design of repeat-accumulate codes for iterative detection and decoding," *IEEE Trans. Signal Process.*, vol. 51, no. 11, pp. 2764–2772, Nov. 2003.

[14] A. Barbieri and G. Colavolpe, "On the information rate and repeat-accumulate code design for phase noise channels," *IEEE Trans. Commun.*, vol. 59, no. 12, pp. 3223–3228, Dec. 2011.

[15] H. Jin, A. Khandekar, and R. McEliece, "Irregular repeat-accumulate codes," in *Proc. IEEE Int. Symp. Turbo Codes and Rel. Topics*, Brest, France, Sep. 2000, pp. 1–8.

[16] S. Benedetto, D. Divsalar, G. Montorsi, and F. Pollara, "Serial concatenation of interleaved codes: performance analysis, design, and iterative decoding," *IEEE Trans. Inf. Theory*, vol. 44, no. 3, pp. 909–926, May 1998.

[17] J. Thorpe, "Low-density parity-check (LDPC) codes constructed from protographs," NASA JPL, Pasadena, CA, USA, IPN Progress Report 42-154, Aug. 2003.

[18] T. Richardson and R. Urbanke, "The capacity of low-density parity-check codes under message-passing decoding," *IEEE Trans. Inf. Theory*, vol. 47, no. 2, pp. 599 – 618, Feb. 2001.

[19] X.-Y. Hu, E. Eleftheriou, and D. Arnold, "Regular and irregular progressive edge-growth Tanner graphs," *IEEE Trans. Inf. Theory*, vol. 51, no. 1, pp. 386–398, Jan. 2005.

[20] M. Davey and D. MacKay, "Low density parity check codes over GF(q)," *IEEE Commun. Lett.*, vol. 2, no. 6, pp. 70–71, Jun. 1998.

[21] F. Kschischang, B. Frey, and H.-A. Loeliger, "Factor graphs and the sum-product algorithm," *IEEE Trans. Inf. Theory*, vol. 47, no. 2, pp. 498–519, Feb 2001.

[22] R. Gallager, *Information theory and reliable communication*. New York, NY, USA: Wiley, 1968.

[23] *Digital Video Broadcasting (DVB); Second Generation Framing Structure, Channel Coding and Modulation Systems for Broadcasting, Interactive Services, News Gathering and Other Broadband Satellite Applications (DVB-S2)*, ETSI EN 302 307 v1.2.1, ETSI European Standard (Telecommunications series), Aug. 2009.